arXiv:1601.02663v2 [cond-mat.mtrl-sci] 11 Mar 2016

Evidence of Landau Level broadening due to strain fluctuations in single-layer graphene

F. M. Ardito,[1] T. G. Mendes-de-Sá,[2] P. F. Gomes,[1,3] D. L. Mafra,[2] R. G. Lacerda,[2] F. Iikawa,[1] and E. Granado[1]

[1]*Instituto de Física "Gleb Wataghin," Universidade Estadual de Campinas, Campinas, São Paulo 13083-859, Brazil*

[2]*Departamento de Física, Universidade Federal de Minas Gerais, Belo Horizonte, Minas Gerais 30123-970, Brazil*

[3]*Instituto de Cincias Exatas e Tecnológicas, Universidade Federal de Goiás, Jataí 75801-615, Brazil*

Abstract

The Landau Level (LL) broadening mechanisms in graphene were investigated through a quantitative analysis of magneto-micro-Raman experiments in two different samples, namely a natural single layer graphene (SLG) flake deposited over a Si/SiO_2 substrate and a multilayer epitaxial graphene (MEG) sample. Interband LL transition widths were extracted from the dampening of the magnetophonon resonances associated with optically active LL transitions crossing the energy of the E_{2g} Raman-active phonon. Our results on the MEG samples are similar to previous reports and consistent with LL energy widths $\propto \sqrt{B}$. On the other hand, SLG shows a much stronger dampening of the low-field resonances that is consistent with an additional broadening mechanism with LL energy widths $\propto 1/\sqrt{B}$. This contribution is argued to be a signature of random strain-induced pseudomagnetic fields that take place in SLG samples and are absent in self-protected MEG.

PACS numbers: 73.22.Lp, 71.70.Di, 78.67.-n, 78.30.Na

The singular half-integer quantum hall effect in graphene is a direct consequence of the characteristic Landau levels (LL) predicted by the Dirac equation. Albeit sharp levels are required to reinforce the manifestation of this effect, little information on the most relevant mechanisms leading to broadening of quantized electronic levels in graphene samples is presently available. The LL energies for the linear electronic bands around the Dirac points in graphene are $E_n = sgn(n)v_F\sqrt{2e\hbar B|n|}$ [1], where the index $n = 0, \pm1, \pm2, ...$, v_F is the Fermi velocity and B is the magnetic field perpendicular to the carbon sheet. Ideal graphene, i.e., a perfectly flat, isolated, defect-free and strain-free layer, is expected to show sharp LLs at low temperatures, with small intrinsic broadening ($\delta E_n \lesssim 1$ meV for $B = 4$ T) due to carrier-carrier, carrier-light and carrier-phonon interactions [2]. On the other hand, real samples show imperfections that are characteristic of the sample production method, leading to LL broadening and consequent dampening of the effects associated to the Dirac equation. A proper understanding of the main mechanisms of extrinsic LL broadening is therefore desirable and should help in the quest for optimized graphene samples with reinforced quantum relativistic effects.

As detailed below, the mechanisms of LL broadening may be pinned down by a quantitative analysis of the B-dependence of the LL width. Such information can be achieved by direct observations of the LL by Scanning Tunelling Spectroscopy [3, 4], Infrared absorption [5–8] and Raman scattering [9, 10]. Alternatively, the broadening of LL may be conveniently studied by an analysis of phonon Raman scattering, which is a versatile and widespread technique that probe structural and electronic properties of graphitic samples. In fact, electron-phonon interaction in graphene leads to magneto-phonon resonances (MPR) when the energy of an optically active LL transition obeying $|n| - |m| = 1$ crosses the energy of the E_{2g} Raman-active phonon [11–13], causing oscillations of the phonon energy and linewidth. Several works have reported the MPR from Dirac fermions in graphene and graphitic samples [9, 14–20]. For electrically neutral graphene, the MPR are described by [14]

$$\widetilde{\epsilon}^2 - \epsilon_0^2 = 4\lambda\epsilon_0 e\hbar B v_F^2 \sum_{k=0}^{\infty}\left[\frac{T_k}{\left(\widetilde{\epsilon} + \imath\delta_k\right)^2 - T_k^2} + \frac{1}{T_k}\right] \tag{1}$$

where ϵ_0 stands for the phonon energy in the absence of magnetic field, λ is the electron-phonon coupling parameter, and $T_k = v_f\sqrt{2e\hbar B}\left(\sqrt{k} + \sqrt{k+1}\right)$ describes the energy of interband LL transitions, with index k, for $|n| - |m| = 1$, in which n and m are labels

for the initial and final Landau levels involved in the transition. δ_k represents the LL broadening parameter, which is of particular significance to the present work. The real and complex parts of $\widetilde{\epsilon} = \epsilon - i\Gamma$ yield the phonon energy and broadening from the electron-phonon coupling, respectively. Comparison between Eq. 1 and the E_{2g} phonon energy and linewidth experimentally obtained as a function of magnetic field allows one to extract sample-related parameters such as v_F, λ and δ_k.

In this work, the MPR of two distinct graphene samples, namely a multilayer epitaxial graphene (MEG) and a single layer graphene (SLG) deposited over a SiO_2 substrate, were quantitatively analysed by means of Eq. 1 in order to extract information on the broadening δ_k parameter. The distinct behavior of δ_k as a function of the resonance index k found for MEG and SLG samples allowed us to identify an additional LL broadening mechanism for SLG not present in MEG layers, associated with random strain due to the interactions with the SiO_2 substrate.

The micro-Raman spectra of our graphene samples were taken using a 488 nm Ar-ion laser and a 15 T magnetocryostat. The sample was fixed to piezoelectric stages. The sample, xyz stages and objective were immersed in He gas or superfluid. The magnetic field was perpendicular to the sample surface. The elastic component of the scattered signal was rejected by an edge filter. For the experiment on multilayer epitaxial graphene on SiC, a 200 μm diameter size optical fiber, which works as a confocal configuration, was used to transport the Raman signal to the entrance of a single 1800 g/mm grating spectrometer coupled with a liquid nitrogen-cooled charge coupled device detector; the laser was focused using a 50X objective lens, with 7 mm working distance and a spot size of ≈ 2.5 μm. For SLG on SiO_2, a single 1200 g/mm grating spectrometer with a peltier-cooled CCD detector was employed; we used a 40$\times$ objective lens with a 200 μm working distance, resulting in ~ 3.5 μm focal spot diameter.

We first investigate the MEG sample. This sample was obtained by decomposition of the carbon face of 4H-SiC$(000\overline{1})$ substrate in argon atmosphere. Sublimation time was 60 minutes at $T = 2048$ K. Further details on the preparation and characterization of this sample by Raman scattering, atomic force microscopy and grazing-incidence x-ray diffraction are given in Ref. [21]. Such samples are known to present weak electronic coupling between graphene layers [22], also showing very small carrier concentrations of the order of 10^{10} cm^{-2} or lower [5, 7]. Sample regions showing graphene-like Raman spectra with sharpest

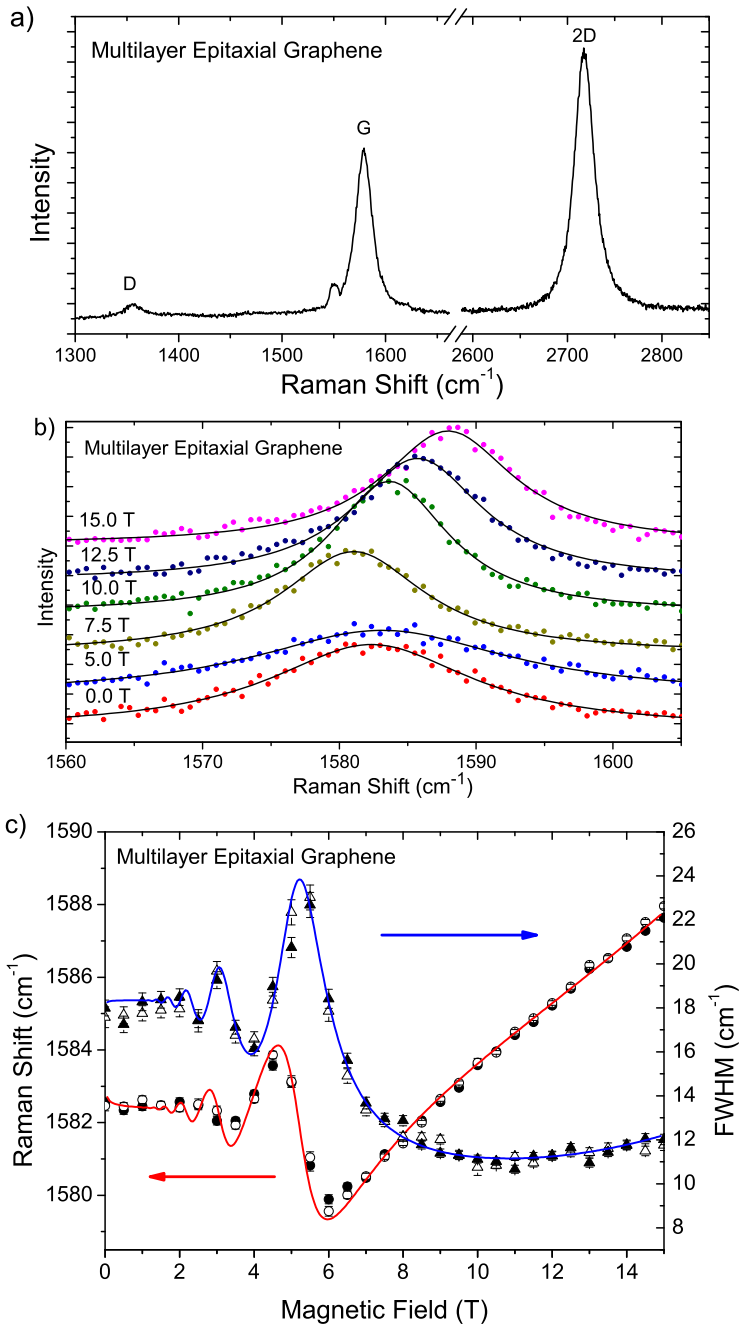

FIG. 1: (a) Raman spectra of multilayer epitaxial graphene on SiC at 5.5 K and zero field. The characteristic graphene D, G, and $2D$ bands are indicated. The peak at ~ 1555 cm^{-1} is a spurious signal due to parasitic scattering in the optical fiber. (b) G-band at selected magnetic fields and $T = 5.5$ K; points represent experimental data and solid lines are lorentzian curve fittings. (c) E_{2g} phonon energy and full width at half maximum (FWHM) as a function of magnetic field; empty and filled circles represents two sets of data, taken on different spots of the sample, both showing a graphene-like single-peaked $2D$ band; solid lines represents a simulation according to Eq. 1 using a single Landau level width $\delta = 17.6$ meV for all inter-LL transitions.

$2D$ bands were chosen for our study. Figure 1(a) shows the overall Raman spectrum at 5 K, showing the characteristic D, G and $2D$ bands. The Raman spectra of this sample nearby the E_{2g} mode (G-band) are displayed in Fig. 1(b) for selected applied magnetic fields, revealing a clear B-sensitivity. Single-lorentzian fits were performed (solid lines in Fig. 1(b)) and the peak energy and linewidth (FWHM) were extracted for two sets of data obtained at distinct spot positions on the sample, yielding reproducible oscillations with field that are signatures of the magneto-phonon resonance in graphene [14] (see Fig. 1(c)). Excellent match with experimental data is obtained if Eq. 1 is employed with the parameters $\epsilon_0 = 1581.7$ cm^{-1}, $v_f = 0.985\times10^6$m/s, $\lambda = 4.1\times10^{-3}$, and $\delta_k = 17.6$ meV for all k (see solid lines in Fig. 1(c)). A constant phonon linewidth contribution $\Gamma_0 = 8.2$ cm^{-1}, attributed to phonon decay processes not related to the electron-phonon coupling, was convoluted with Γ to model the total B-dependent linewidth of the $G-$band. Overall, the extracted parameters are comparable to those previously reported for another MEG sample [14].

We proceed to the investigation of a SLG flake, produced by conventional mechanical exfoliation of natural graphene deposited over the 300 nm SiO_2 layer of a Si substrate. Figure 2(a) shows the optical image of this sample. Figure 2(b) shows the overall Raman spectrum at room temperature with the characteristic G and $2D$ bands and no sign of the defect-activated D-band. This result indicates absence of a significant level of structural defects such as atomic vacancies or impurities. A combined analysis of the peak intensities [23], areas [24], positions and linewidths [23, 25] of the G- and $2D$- bands extracted from the room-temperature Raman spectrum reveals an electrically neutral graphene within our resolution ($n_0 = 0 \pm 1 \times 10^{12}$ cm^{-2}). The G-band Raman spectrum for selected magnetic fields and $T = 5$ K is displayed in Fig. 2(c). This band clearly splits in two peaks above ~ 12 T, in line with previous reports [18, 26]. Figure 3 shows the position of the G-band at 5 K as a function of magnetic field. For $B \lesssim 12$ T, where a single G-band was observed within our resolution, no magnetophonon resonance could be detected, in contrast to the MEG sample. For $B > 12$ T, one of the components of the splitted $G-$band remain at a nearly constant energy position, while a second component follows a pre-resonant behavior associated with the $k = 1$ ($n = 0 \leftrightarrow \pm1$) inter-Landau level transitions at $B_{res}^{k=1} = 25 - 30$ T [18]. Note that the peak position of this field-dependent component follows a similar behavior found for the MEG sample in the higher-field regime above 12 T (see also Fig. 1(c)). It is therefore evident from our results and from the literature [18, 26] that SLG on

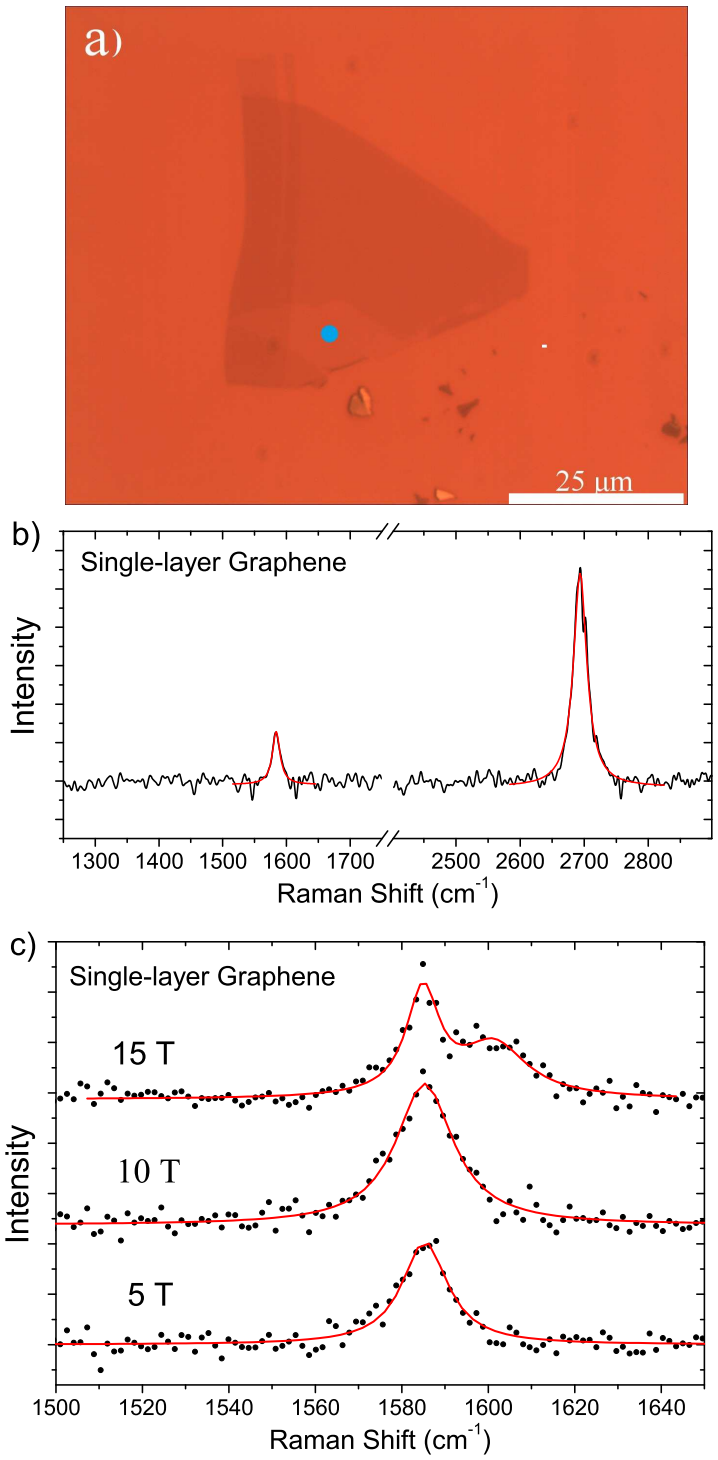

FIG. 2: (a) Optical image of our exfoliated graphene sample, obtained using an orange filter. The blue circle indicates the approximate dimension and position of the laser spot focused into the single-layer graphene (SLG) region. (b) Raman spectrum of the SLG region at room temperature. The G and $2D$ bands are observed at 1584 and 2694 cm^{-1} with full widths at half maxima of 14.3(9) and 25.4(3) cm^{-1}, respectively. The $2D/G$ peak area and peak heigth ratios are 7.2(5) and 4.1(3), respectively. (c) G-band of the SLG sample at $T = 2$ K and various magnetic fields. Solid lines in (b) and (c) are lorentzian fits to the observed peaks.

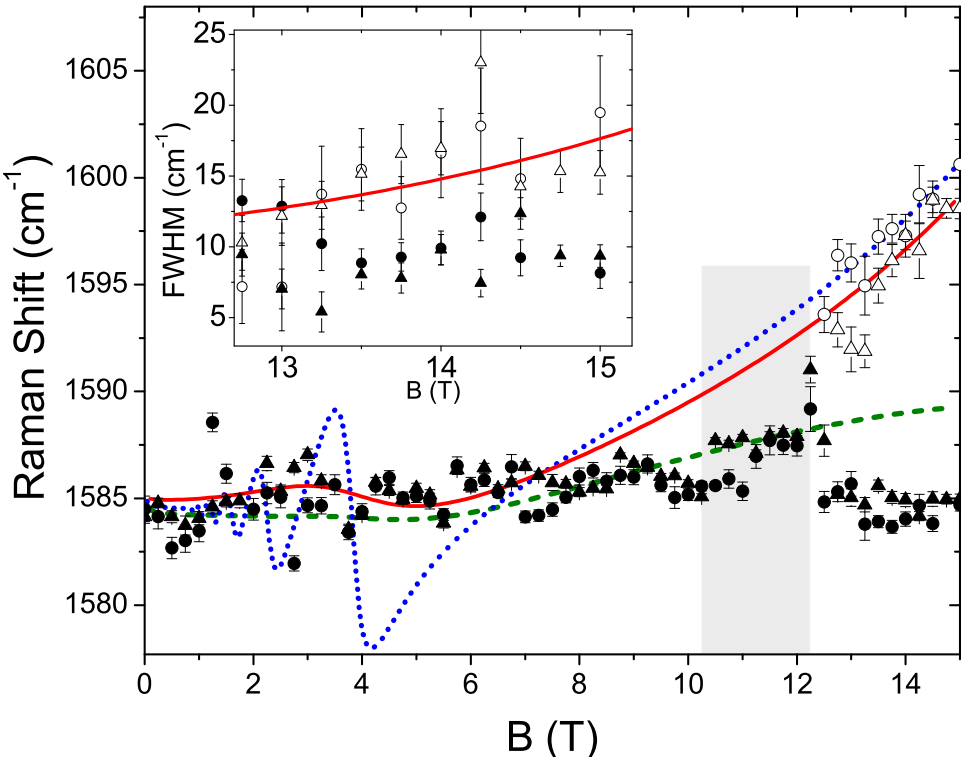

FIG. 3: $G-$band central positions for the single layer graphene sample, obtained by fits using a single lorentzian below 12 T and two lorentzians above 12 T (see also Fig. 2(c)). The grey area marks an intemediate field region where a single peak was employed in the fit although a double peak structure, not resolved in our data, is likely to be present. Circles and triangles refer to datasets taken on two independent runs. The results for the B-dependent component above 12 T are given as open symbols. Dashed green and dotted blue lines are the simulated magnetophonon resonance effect according to Eq. 1 using fixed Landau level broadening parameters $\delta = 13.6$ and 63 meV, respectively. The inset shows the $B-$dependence of the full width at half maxima for the two peaks observed above 12 T (symbols). The solid red lines in the main panel and in the inset are the results of a simulation using Eq. 1 with δ parameter dependent on B using $\Delta B = 1.7$ T and $\delta_0 = 6.3$ meV (see text).

SiO_2 is inhomogeneous and regions with two distinct behavious are found within probed areas of a few μm^2: (i) regions showing no observable magnetophonon resonance at all and (ii) regions showing clear manifestations of the main $k = 0$ resonance.

Insight into the observed behavior of the G-band with field for single-layer exfoliated graphene on SiO_2 is gained by an analysis of Eq. 1 as a function of the δ_k parameters related

to the LL transition widths. The dashed and dotted lines in Fig. 3 show the calculated B-dependence of the G-band central wavenumber for two selected values of δ, assumed so far to be the same for all transition indexes k. In these simulations, the parameters $\epsilon_0 = 1582$ cm^{-1}, $v_f = 1.15 \times 10^6$ m/s, $\lambda = 5.5 \times 10^{-3}$ were employed. For $\delta = 13.6$ meV, the high-field pre-resonant behavior observed for one of the $G-$band components is captured. However, if the same δ is used for the other LL transitions, the resonance at 3.8 T associated to the $n = -1 \rightarrow 2$ and $n = -2 \rightarrow 1$ LL transitions remains proeminent and would be clearly visible within our resolution. If, on the other hand, a much larger $\delta = 63$ meV is employed in the simulations, all the magnetophonon resonances are washed out, including the observed pre-resonant behavior in the field range $B >$12 T. We conclude that, while the $B-$independent component of the $G-$band observed in single-layer graphene on SiO_2 may be attributed to sample regions showing a very large δ value, the behavior observed for the $B-$dependent $G-$band component cannot be explained by single-δ magnetophonon resonances. In fact, a much larger δ_k for the low-field resonances ($k \geq 2$) with respect to the main one ($k =$1) is necessary for Eq. 1 to capture the observed behavior of the $B-$dependent G-band component of our single-layer graphene sample. This conclusion is not restricted to our exfoliated single-layer sample on SiO_2. In fact, recent results of magnetophonon resonance on single-layer graphene encapsuled on hexagonal boron nitride by Neumann *et al.* could only be fit with increasing δ_k parameters with k [20].

In summary, the experimental data indicate that for MEG the LL broadening parameter δ_k in the magnetophonon resonance (eq. 1) is actually independent of k, while for SLG δ_k increases with k. We proceed with a discussion on the significance of these observations. As mentioned above, the manifestations of MPR in the Raman spectra occur at fields (B^k_{res}) where the interband LL energy difference equals the $G-$band energy, i.e., $E_{G-band} = v_F\sqrt{2e\hbar B^k_{res}}(\sqrt{|n|} + \sqrt{|n+1|})$. In other words, in this experiment distinct LL transitions are "seen" at the same energy but different magnetic fields. The observation of a LL broadening parameter δ that is independent of the transition index k indicates that the LL width is proportional to its energy. Since the LL energy is in turn proportional to $\sqrt{B}$, this conclusion is consistent with direct measurements of LL widths as a function of B for MEG samples, where a $\sqrt{B}$-dependence is found for the LL widths [7, 8]. Recent theoretical work analysed different microscopic mechanisms of LL broadening and attributed this $\sqrt{B}$-dependence to an extrinsic mechanism involving scattering of the charge carriers by im-

purities [2]. In fact, intrinsic mechanisms such as scattering from carrier-carrier, carrier-light and carrier-phonon interactions cannot explain the relatively large LL broadening observed for MEG ($\delta_k/E_k = 0.09$ for our sample). We should mention that an additional extrinsic mechanism of LL broadening involving fluctuations of v_F from layer to layer may also lead to the same behavior with constant δ_k/E_k ratio, since the LL energy is proportional to v_F. In fact, it is well established that v_F is dependent of a residual interaction with the substrate or neighboring graphene layers, reaching maximum values for suspended single-layer graphene samples [32], making Fermi velocity fluctuations a plausible source of LL broadening in MEG.

For SLG, it is evident that an additional extrinsic mechanism must be present to account for the index-dependent broadening that washes out the resonances with $k \geq 2$. In fact, while for MEG samples the graphene layers are self-protected, for SLG the interaction with the substrate is significant. The most plausible influence of the substrate in the LL structure of graphene is through the induction of strain fluctuations associated with corrugation of the graphene layer.

In the absence of a complete microscopic theory that takes into account the effect of inhomogeneous strain in the LLs of graphene, we propose a phenomenological approach that seems to capture the essential physics. It is well known that strain leads to a discretization of the electronic levels in graphene that are similar to the effect of an external magnetic field [1, 29, 30]. Since strain in SLG over SiO_2 substrates is inhomogeneous, it is expected that a distribution of pseudo-magnetic fields takes place, which would introduce a certain standard deviavion ΔB in the effective magnetic field and lead to an obvious pathway to LL broadening. Quantitatively, one would have $\Delta E_n/E_n = \Delta B/2B$, and therefore $\Delta E_n \propto 1/\sqrt{B}$.

In order to verify if broadening mechanisms indicated above are consistent with our observations in SLG, simulations of the E_{2g} phonon energy and linewidth according to Eq. 1 were performed considering the Lorentzian-convoluted parameter $\delta_k = \delta_0 + (\Delta B/2B^k_{res})E_{G-band}$, where the $k-$independent term δ_0 accounts for the combined effect of impurity scattering and Fermi velocity distribution. Good match with experimental data for the $B-$dependent component of the G-band is found using the parameters $\delta_0 = 6.3$ meV and $\Delta B = 1.7$ T (solid lines in Fig. 3 and inset). This good match strongly suggest that the LL broadening that damps the resonances at low fields in SLG indeed arises from a large local pseudo-

magnetic field distribution created by interactions with the substrate [1, 29, 30]. Indeed, it is known that such pseudo-magnetic fields could reach values up to tens of tesla in some cases [31], therefore the observed value of $\Delta B = 1.7$ T for our SLG sample on SiO_2 is a reasonable result.

In conclusion, a comparative and quantitative analysis of the magneto-phonon resonances in MEG and SLG samples allowed us to identify an extrinsic LL broadening mechanism for single layer (and possibly few-layer) graphene associated with strain caused by interactions with the substrate. This work suggests that systematical investigations of extrinsic Landau level broadening mechanisms for graphene can be done using Raman spectroscopy, providing a relatively straightforward methodology to probe carrier scattering channels that could guide optimization of graphene production methods.

We thank M.A. Pimenta, E. Nery, F. Plentz, and L. Malard for helpful discussions. This work was supported by CAPES, FAPESP, FAPEMIG, CNPq, Nanocarbon INCT and Nanofabrication Network, Brazil.

[1] A.H. Castro Neto *et al.*, Rev. Mod. Phys. **81**, 109 (2009).

[2] H. Funk, A. Knorr, F. Wendler, and E. Malic, Phys. Rev. B **92**, 205428 (2015).

[3] G. Li, A. Luican, and E.Y. Andrei, Phys. Rev. Lett. **102**, 176804 (2009).

[4] A. Luican-Mayer *et al.*, Phys. Rev. Lett. **112**, 036804 (2014).

[5] M.L. Sadowski *et al.*, Phys. Rev. Lett. **97**, 266405 (2006).

[6] Z. Jiang *et al.*, Phys. Rev. Lett. **98**, 197403 (2007).

[7] M. Orlita *et al.*, Phys. Rev. Lett. **101**, 267601 (2008).

[8] M. Orlita *et al.*, Phys. Rev. Lett. **107**, 216603 (2011).

[9] C. Faugeras *et al.*, Phys. Rev. Lett. **107**, 036807 (2011).

[10] C. Faugeras *et al.*, Europhys. Lett. **108**, 27011 (2014).

[11] T. Ando, J. Phys. Soc. Japan, **74**, 777 (2005).

[12] T. Ando, J. Phys. Soc. Japan **76**, 024712 (2007).

[13] M.O. Goerbig, J.-N. Fuchs, K. Kechedzhi, and V.I. Fal'ko, Phys. Rev. Lett. **99**, 087402 (2007).

[14] C. Faugeras *et al.*, Phys. Rev. Lett. **103**, 186803 (2009).

[15] J. Yan *et al.*, Phys. Rev. Lett. **105**, 227401 (2010).

[16] Y. Kim *et al.*, Phys. Rev. B **85**, 121403 (2012).

[17] S. Goler, J. Yan, V. Pellegrini, and A. Pinczuk, Sol. State Commun. **152**, 1289 (2012).

[18] Y. Kim *et al.*, Phys. Rev. Lett. **110**, 227402 (2013).

[19] P. Leszczynski *et al.*, Nano Lett. **14**, 1460 (2014).

[20] C. Neumann *et al.*, Nano Lett. **15**, 1547 (2015).

[21] T.G. Mendes-de-Sá *et al.*, Nanotechnol. **23**, 475602 (2012).

[22] C. Faugeras *et al.*, Appl. Phys. Lett. **92**, 011914 (2008).

[23] A. Das *et al.*, Nature Nanotech. **3**, 210 (2008).

[24] D.M. Basko, S. Piscanec, and A.C. Ferrari, Phys. Rev. B **80**, 165413 (2009).

[25] S. Pisana *et al.*, Nature Mater. **6**, 198 (2007).

[26] S. Remi, A. Swan, and B.B. Goldberg, *in Proceedings of the XXII International Conference on Raman Spectroscopy*; editors: P. M. Champion and L. D. Ziegler, p. 465 (2010).

[27] L.M. Malard *et al.*, Phys. Rev. B **76**, 201401 (2007).

[28] M.A. Pimenta *et al.*, Phys. Chem. Chem. Phys. **9**, 1276 (2007).

[29] T. Ando, J. Phys. Soc. Japan **75**, 124701 (2006).

[30] A.F. Morpurgo and F. Guinea, Phys. Rev. Lett. **97**, 196804 (2006).

[31] N.-C. Yeh, N.-C. *et al.*., Surf. Science **605**, 1649 (2011).

[32] C. Hwang *et al.*, Sci. Rep. **2**, 590 (2012).